Analytical description of the evolution of polarized light in homogeneous retarders using Jones formalism

C. Ayala Díaz
Facultad de Ingeniería Ensenada, Universidad Autónoma de Baja California,
km 103 carretera Tijuana-Ensenada, Ensenada, B.C., 22860 México,
Tel. (646)-175-0744,
e-mail: ayala@uabc.mx

D. Tentori Santa Cruz
Departamento de Óptica, División de Física Aplicada,
Centro de Investigación Científica y de Educación Superior de Ensenada,
km 107 carretera Tijuana-Ensenada, Ensenada, B.C., 22860 México,
Tel. (646)-175-0500 Ext. 25035,
e-mail: diana@cicese.mx

M. Avendaño Alejo
Centro de Ciencias Aplicadas y Desarrollo Tecnológico, Universidad Nacional Autónoma de México,
Circuito Exterior S/N, Ciudad Universitaria, México, D.F., 04510 México,
Tel. (55)-5622-8602 Ext. 1121,
e-mail: maximino.avendano@ccadet.unam.mx

Recibido el 13 de noviembre de 2008; aceptado el 27 de mayo de 2009

In this work we present analytical expressions for the trajectories depicted in the complex plane by the evolution of the state of polarization of totally polarized light, as it propagates through a homogeneous retarder. For any retarder and input state of polarization of the signal, the polarization state evolves, depicting one circle on the complex plane. The radius and position of each circle depends on the orientation of the fast birefringence axis of the sample, the polarization state of the input signal and the specific anisotropy of the medium.

Keywords: Birefringence; Jones matrices; polarization.

En este trabajo se presentan expresiones analíticas de las trayectorias descritas en el plano complejo, cuando el estado de polarización de una señal completamente polarizada evoluciona al propagarse por un retardador homogéneo. Para cada retardador y cada estado de polarización de la señal de entrada, el estado de polarización evoluciona describiendo un círculo en el plano complejo. El radio y la posición de cada círculo dependen de la orientación del eje rápido de la birrefringencia de la muestra, del estado de polarización de la señal de entrada y de la anisotropía

Descriptores: Birrefringencia; matrices de Jones; polarización.

PACS: 02.60Dc; 42.81.Gs

1. Introduction

In practical applications homogeneous retarders are very important since the residual birefringence of a short length of a non-spun single-mode fiber with negligible absorption as well as the intrinsic birefringence of a nematic liquid crystal can be described as media with homogeneous retardation. Due to its anisotropy, the observable variations of the output polarization state of a polarized signal propagated through these media depend strongly upon experimental conditions such as input polarization and sample length [1-3]. To analyze the birefringence of a sample or to design a specific device, the position, form, and sense of the ellipse described by the light vector must be determined at each point of the light trajectory. In order to simplify the analysis when the medium birefringence is not known or to model it for design purposes, graphic methods can be used [4-6].

Graphic methods are based on the use of the trajectories depicted by the evolution of light polarization as it propagates through media with a known anisotropy [4-6]. Such trajectories represent exact solutions of the coupled wave equations, particularly relevant for the new anisotropic media used in optoelectronics and guided optics.

Since its introduction, Jones-matrix theory has been a powerful tool for dealing with polarization components and systems, being the main formalism applied to describe the polarization optics of guided light systems and devices. In this work we apply Jones matrix theory and the polarization complex-plane to model the polarization performance of homogeneous anisotropic media with a single propagation direction, such as optical fibers or liquid crystal cells. In this complex-plane the polarization state is represented using the E_y to E_x ratio of the electric vector components [7-12]. The real part of this quotient corresponds to the x axis and the

imaginary part to the y axis. This representation is equivalent to the Poincaré sphere description, having the advantage when working with Jones matrix formalism that it does not require the use of a second formalism and that the graphical analysis can be performed on a flat sheet of paper. This work is organized as follows: Sec. 2 introduces the complex plane representation; Secs. 3, 4 and 5 present the mathematical description of the trajectories described by the evolution of the state of polarization along homogeneous retarders for linear, circular and elliptical birefringence, respectively. For each kind of homogeneous retarder two types of input or output polarized signals are considered, linear and circular; Sec. 6 resumes the results; finally, Sec. 7 presents our conclusions.

2. Complex-plane mapping

The state of polarization of light can be represented on a plane using graphic descriptions different from those used in this work [13-16]. We utilize the stereographic projection [7-12] based on the ratio of the x and y components of the electric field vector:

$$\mathbf{E} = A_x e^{i(\omega t - \phi_x)}\mathbf{i} + A_y e^{i(\omega t - \phi_y)}\mathbf{j}. \tag{1}$$

Removing its temporal dependence,

$$\mathbf{E} = E_x\mathbf{i} + E_y\mathbf{j} = A_x e^{-i\phi_x}\mathbf{i} + A_y e^{-i\phi_y}\mathbf{j} \tag{2}$$

and choosing the origin of the phases on the linear component, parallel with the positive branch of x-axis, the complex ratio of the y to x components is

$$\frac{E_y}{E_x} = \left(\frac{A_y}{A_x}\right) e^{i\Delta}, \tag{3}$$

where Δ = ϕ_y - ϕ_x[7,12]. As we can see, this complex ratio replaces absolute amplitudes and phases by relative quantities.

Transforming Eq. (3) in its trigonometric equivalent

$$\frac{E_y}{E_x} = \left(\frac{A_y}{A_x}\right)\cos\Delta + i\left(\frac{A_y}{A_x}\right)\sin\Delta = u + iv, \tag{4}$$

the state of polarization is mapped on a complex-plane defined by the coordinate axes u and v [7-12]. This graphical description has been used to represent those states that share the same azimuth or ellipticity [17] and to outline the shape of the trajectories describing the polarization evolution of light along several anisotropic media [5]. In what follows we calculate the analytical relations that describe the evolution of polarized light along homogeneous retarders (linear, circular and elliptical) and show how this information is related to the birefringence of a sample and with the polarization state of the input signal.

3. Linear birefringence

Our interest is focused on single-mode optical fibers. Due to its dimensions and symmetry, the alignment of the birefringence axis with the reference frame used to measure the state of polarization is not obvious. Therefore, to describe the birefringence of the medium we use a Jones matrix in which the fast birefringence axis is not aligned with the x axis of the reference system. In this case, the birefringence matrix of a linear retarder is

$$M_L = \begin{bmatrix} \cos\frac{\delta}{2} + i\sin\frac{\delta}{2}\cos 2\alpha & i\sin\frac{\delta}{2}\sin 2\alpha \\ i\sin\frac{\delta}{2}\sin 2\alpha & \cos\frac{\delta}{2} - i\sin\frac{\delta}{2}\cos 2\alpha \end{bmatrix}, \tag{5}$$

where δ is the retardation angle between polarization eigenmodes and α is the azimuth angle of the fast birefringence axis [6-8].

Circular input polarization

We will describe a circularly polarized input signal as

$$\mathbf{V}_C = \begin{bmatrix} 1 \\ \pm i \end{bmatrix}, \tag{6}$$

where the positive sign corresponds to a left circular polarization and the negative sign corresponds to a right circular polarization. Using Jones formalism, the output state of polarization is

$$\mathbf{V}_{out} = \mathbf{M}\mathbf{V}_{in}. \tag{7}$$

From Eqs. (5), (6) and (7), the output polarization state for a linear retarder illuminated with a circular signal is

$$V_{LC} = \begin{bmatrix} \cos\left(\frac{\delta}{2}\right) \mp \sin 2\alpha \sin\left(\frac{\delta}{2}\right) + i\sin\left(\frac{\delta}{2}\right)\cos 2\alpha \\ \pm\sin\left(\frac{\delta}{2}\right)\cos 2\alpha + i\left[\sin 2\alpha \sin\left(\frac{\delta}{2}\right) \pm \cos\left(\frac{\delta}{2}\right)\right] \end{bmatrix}. \tag{8}$$

Using Eqs. (4) and (8), the complex plane coordinates of the output signal are

$$u_{LC} = \pm\frac{\sin\delta\cos 2\alpha}{1 - \sin\delta\sin 2\alpha},$$
$$v_{LC} = \pm\frac{\cos\delta}{1 - \sin\delta\sin 2\alpha}. \tag{9}$$

Using these values [Eq. (9)] we calculated the trajectories depicted by the evolution of the state of polarization when the retardation angle δ, between the polarization eigenmodes, varies from 0 to 360° (Fig. 1).

The radii of curvature of the resultant family of circles satisfy

$$r_{LC} = \frac{1}{\cos 2\alpha}, \tag{10}$$

and every circle is centered on a point (h,k) located on the u axis,

$$(h,k)_{LC} = (\tan 2\alpha, 0). \tag{11}$$

In this case the coordinates of the center of the circle match the location of one of the polarization eigenmodes of the sample.

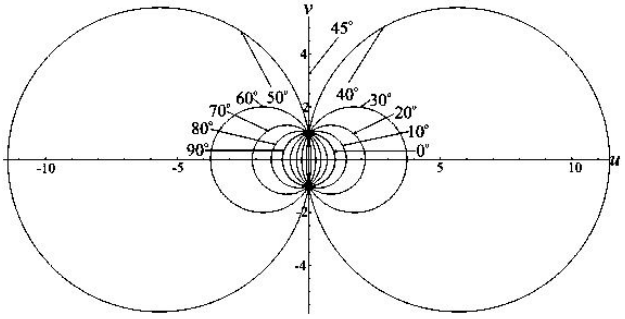

FIGURE 1. Linear retarder illuminated with a circularly polarized input signal. For a sample with the fast birefringence axis angle $\alpha < 45^\circ$ the abscissas of the centers of the circular trajectories are positive, while for $\alpha < 45^\circ$ they are negative.

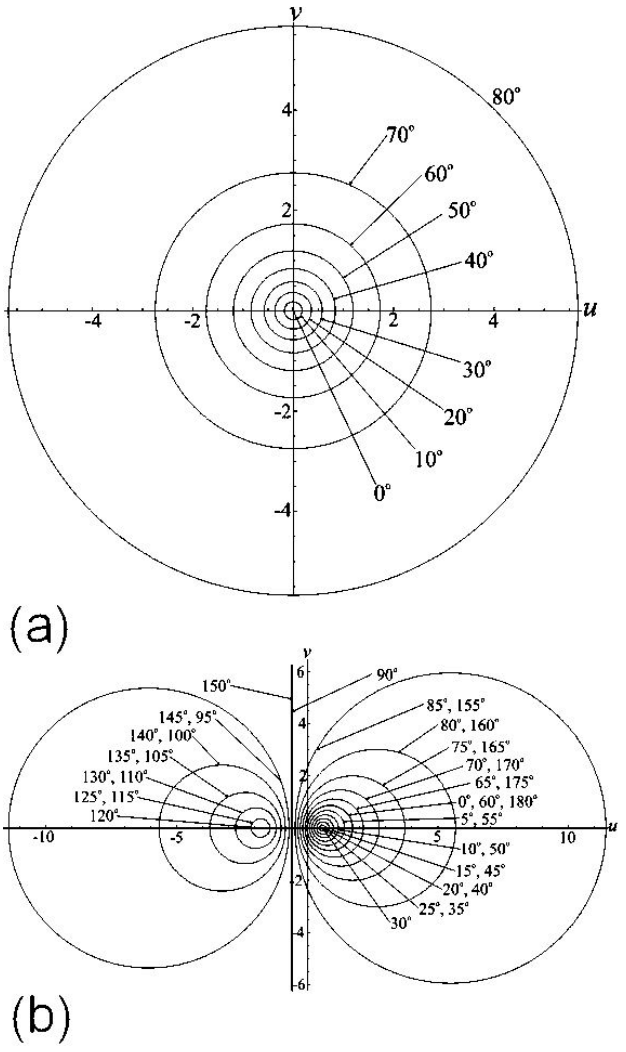

FIGURE 2. a) Sample with fast birefringence axis angle $\alpha = 0^\circ$ and variable azimuth angle (φ) of the linear input signal. As $\varphi \to 90$ or 270°, the radius tends to infinity. b) Sample with fast birefringence axis angle $\alpha = 30^\circ$ and variable orientation of the linear input signal (azimuth angle $0 < \varphi < 180^\circ$).

In Fig. 1 each circle corresponds to a different value of the azimuth angle α of the fast birefringence axis of the sample. Using Eqs. (9)-(11) we can verify that for $\alpha = 0$, the circular trajectory is centered at the origin and has a unitary radius; by contrast, when α approaches $\pm 45^\circ$ (vertical polarization state), the value of the radius goes off to infinity. For a circular input polarization, the radius and the position of the circular trajectory on the complex plane are determined by the azimuth angle of the fast birefringence axis.

Linear input polarization

The trajectories depicted by the evolution of the state of polarization when the input signal is linearly polarized are calculated as follows: the Jones vector of a linearly polarized input signal with azimuth angle φ is [7]:

$$\mathbf{V}_L = \begin{bmatrix} \cos\varphi \\ \sin\varphi \end{bmatrix}. \tag{12}$$

Applying Eq. (7), the output polarization state is given by

$$\mathbf{V}_{LL} = \begin{bmatrix} \cos(\delta/2)\cos\varphi + i\sin(\delta/2)\cos(\varphi - 2\alpha) \\ \cos(\delta/2)\sin\varphi - i\sin(\delta/2)\sin(\varphi - 2\alpha) \end{bmatrix}; \tag{13}$$

therefore, the complex-plane coordinates are in this case

$$\begin{aligned} u_{LL} &= \frac{\sin^2(\delta/2)\sin[2(2\alpha-\varphi)] + \cos^2(\delta/2)\sin 2\varphi}{2[\cos^2(\delta/2)\cos^2\varphi + \sin^2(\delta/2)\cos^2(2\alpha-\varphi)]}, \\ v_{LL} &= \frac{\sin\delta\sin[2(\alpha-\varphi)]}{2[\cos^2(\delta/2)\cos^2\varphi + \sin^2(\delta/2)\cos^2(2\alpha-\varphi)]}. \end{aligned} \tag{14}$$

Using the expressions in Eq. (14) to depict the evolution of the state of polarization of the input linear signal, we obtain again a family of circles (Figs. 2 and 3). In this case their radii are related to the value of the azimuth α of the fast birefringence axis of the material and the azimuth angle φ of the input linear polarization,

$$r_{LL} = \frac{\sin[2(\alpha - \varphi)]}{2\cos\varphi\cos(2\alpha - \varphi)}, \tag{15}$$

and their centers of curvature are located in

$$(h,k)_{LL} = \left(\frac{\sin 2\alpha}{2\cos\varphi\cos(2\alpha - \varphi)}, 0\right). \tag{16}$$

Equation (16) indicates that the centers of these circles lie on the u axis, the real axis. This axis corresponds to electric vectors with linear polarization state and to the polarization eigenmodes of the linear retarder, but in general Eq. (16) does not correspond to the sample eigenmode.

To understand how the evolution of the state of polarization is modified for a linear retarder whose relative orientation with respect to the reference system remains fixed when the azimuth angle of the input linear polarization varies, we calculated the trajectories for $\alpha = 0^\circ$. A set of results is shown in Fig. 2a. When $\varphi = 0^\circ$ (or 180°), $r = 0$; *i.e.* the trajectory would be represented by a point located at the origin of coordinates, one of the eigenmodes of this anisotropic medium.

In this Fig. 2a the trajectories are circles centered at the origin. The value of their radii depends on the value of the azimuth angle of the linear input polarization state. Using Eq. (15) it can be shown that in this case $r = \tan\varphi$; therefore, as φ approaches $\pm 90^\circ$, the radius tends to infinity.

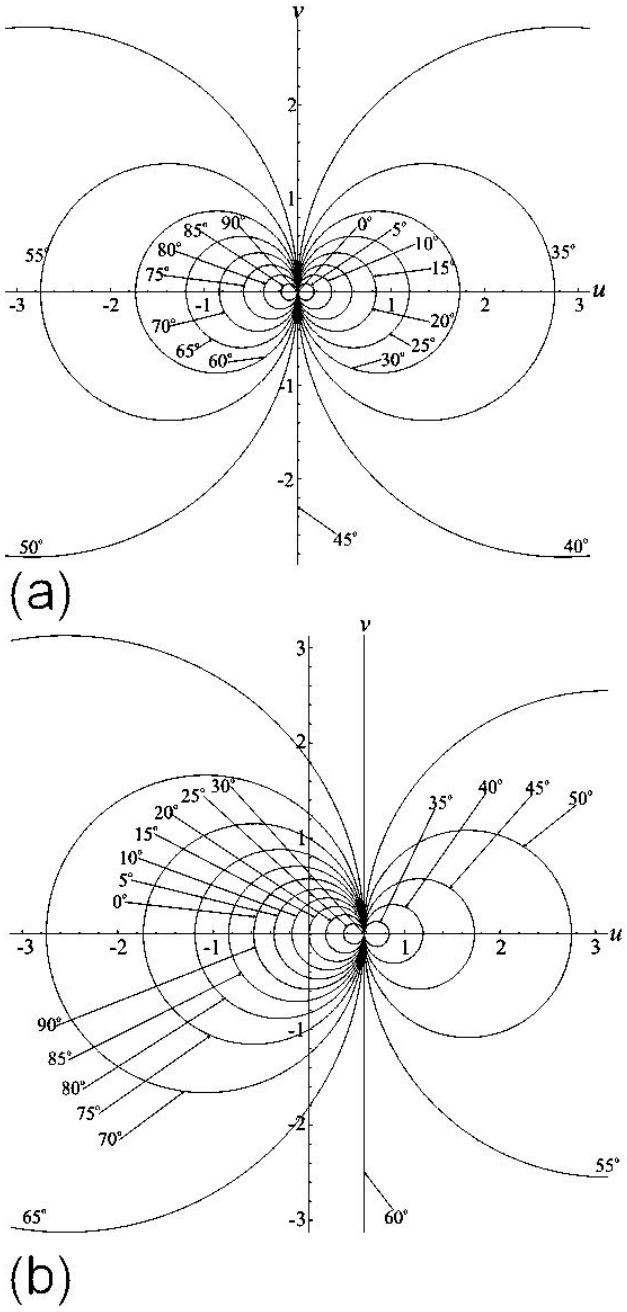

FIGURE 3. a) Linear retarder illuminated with a fixed linear input polarization (φ = 0). Different orientations of the sample were considered. Circles on the right side correspond to $\alpha < 45°$ and those on the left side to $\alpha > 45°$. b) Linear retarder with variable orientation of the fast birefringence axis, $0 < \alpha < 180°$. The input signal has a fixed linear polarization ($\varphi = 30°$).

When the birefringence fast axis is not aligned with the x axis of the reference system, the center of the circle is not located at the origin of coordinates [Eq. (16)]; an example is shown in Fig. 2b for $\alpha = 30°$ and $0° < \varphi < 180°$.

A different practical condition corresponds to cases in which the orientation of the linear retarder varies with respect to the reference frame, and the azimuth angle of the linear polarization state at the sample input remains fixed. In Fig. 3a we show a family of circles obtained for $\varphi = 0°$ and several values of α ranging from 0 to 90°. As we can see, the distribution is symmetric. Trajectories on the right side ($u > 0$) correspond to $\alpha < 45°$ and those on the left side to $\alpha > 45°$. The symmetry is broken when $\varphi \neq 0°$. In Fig. 3b we present the trajectories calculated for $\varphi = 30°$ when $0° < \alpha < 180°$.

Elliptical input polarization

The Poincaré sphere is a particularly useful tool to describe the performance of the anisotropic non-absorbing media considered in this work. Using this representation, the evolution of the state of polarization of light as it propagates through a homogeneous retarder is very easily described using the symmetry properties of this sphere. The resultant circular path represents, at each point of the light trajectory, the position, the form and the direction of the ellipse described by the light vector. The alternative complex plane representation we apply in this work is a stereographic projection of the Poincaré sphere; in this model we map circles onto the sphere as circles in the complex plane [10]. Making use of this fact, for any specific homogeneous linear retarder (specific orientation with respect to the reference system) and input polarization state, there is only one circular path that describes the evolution of the state of polarization of light. This circle includes all the states of polarization through which the light signal may evolve, and any of these states might be used as the input or the output polarization state.

To exemplify the previous reasoning let us consider the trajectory in Fig. 2a, with unitary radius, that includes right and left circular polarizations. In this figure the fast birefringence axis of the linear retarder is aligned with the $x-$axis of the reference system ($\alpha = 0°$) and the azimuth angle of the

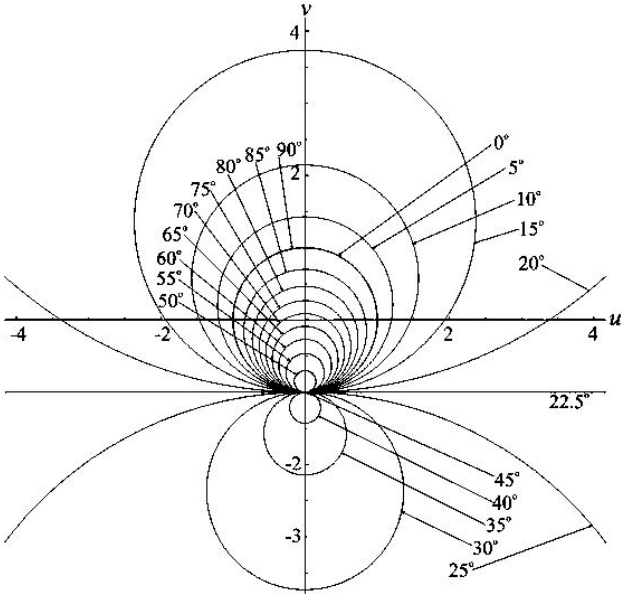

FIGURE 4. Elliptical retarders aligned with the laboratory reference frame ($\alpha = 0°$). Each one has a different ellipticity angle ($0 < \varepsilon < 90°$).The input signal is circularly polarized to the left.

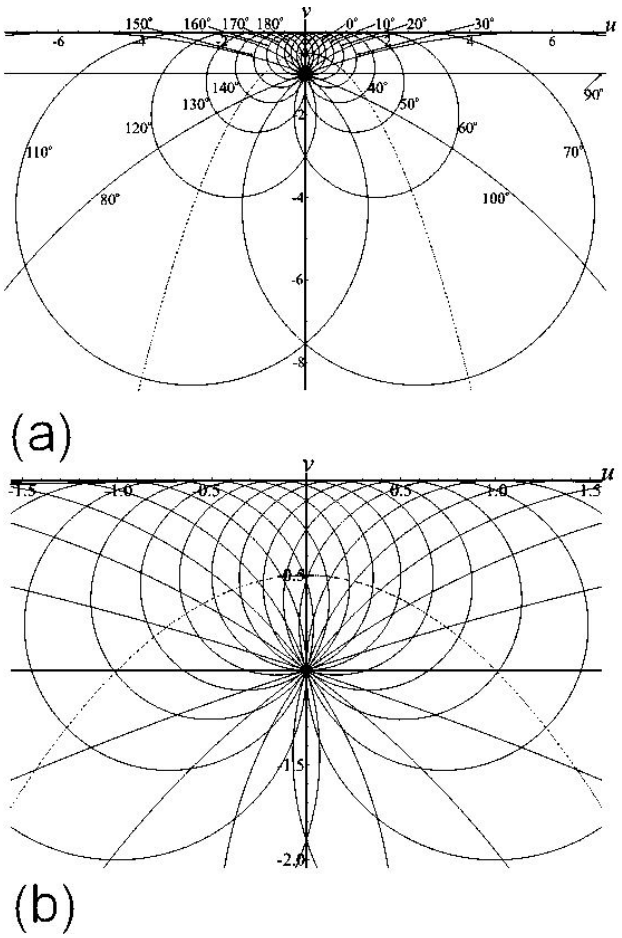

FIGURE 5. a) Elliptical retarder with ellipticity angle ε = 22.5°. The input signal has a left circular polarization. These trajectories were calculated varying the azimuth angle α of the sample from 0 to 180°. b) It is an amplification of Fig. 5a, it helps to visualize the evolute (dashed line) and the envelope (real axis) of this family of circles. The evolute is a parabola whose focus coincides with the input state of polarization.

input linear state of polarization is $\varphi = \pm 45°$. We can notice that this circular trajectory is also illustrated in Fig. 1, corresponds to a linear retarder with zero azimuth angle and in this case, input circular polarization. This input polarization state evolves, becoming a linear polarization state with azimuth angle $\varphi = \pm 45°$. This geometric property, widely used with the Poincaré sphere representation, can also be applied to the present stereographic projection to include any initial elliptical polarization located in this circular trajectory. For any of the elliptical polarization states matching this circular path, this circle describes its evolution along the linear retarder for this specific orientation of the sample with respect to the reference system. Figure 2a reveals that varying the radius of the circular path any elliptical polarization can be considered as input polarization state.

When the azimuth angle of the linear retarder is not aligned with the horizontal axis of the reference system ($\alpha \neq 0°$), the same property can be applied. Using relations (15) and (16) and the sample orientation (azimuth angle α), the circular path that includes the specific elliptical polarization state in which we are interested, can be selected by varying the value of φ. In particular, for the case previously discussed, using Eqs. (15) and (16) it can be shown that Eqs. (10) and (11) give rise to the same circular trajectories when $\varphi = \alpha \pm 45°$.

The use of circular paths obtained for a circular input polarization does not allow any elliptical state of polarization to be considered. For a specific orientation of the sample there is only one circular trajectory including right and left circular states of polarization.

4. Circular birefringence

The birefringence matrix of a circular rotator is:

$$\mathbf{M}_C = \begin{bmatrix} \cos\frac{\delta}{2} & \mp\sin\frac{\delta}{2} \\ \pm\sin\frac{\delta}{2} & \cos\frac{\delta}{2} \end{bmatrix}, \tag{17}$$

where δ is the retardation angle between the polarization eigenmodes. The upper sign corresponds to a left rotator and the lower sign to a right rotator [6,8].

4.1. Circular input polarization

The output polarization state is obtained from Eqs. (6), (7) and (17)

$$\mathbf{V}_{CC} = \begin{bmatrix} \cos\frac{\delta}{2} - i\sin\frac{\delta}{2} \\ \pm\sin\frac{\delta}{2} \pm i\cos\frac{\delta}{2} \end{bmatrix} \tag{18}$$

and, using Eq. (18), it can be shown that, as in agreement with polarization optics,

$$\begin{aligned} u_{CC} &= 0, \\ v_{CC} &= \pm 1, \end{aligned} \tag{19}$$

since right and left circular polarizations are the polarization eigenmodes of a circular rotator. Equation (19) states that the polarization eigenmodes propagate along the sample maintaining the same polarization state.

4.2. Linear input polarization

In this case, using Eqs. (7), (12) and (17) we obtain for the output polarization state

$$\mathbf{V}_{CL} = \begin{bmatrix} \cos\varphi\cos\frac{\delta}{2} \mp \sin\varphi\sin\frac{\delta}{2} \\ \pm\cos\varphi\sin\frac{\delta}{2} + \sin\varphi\cos\frac{\delta}{2} \end{bmatrix}, \tag{20}$$

and from relations 4 and 20

$$\begin{aligned} u_{CL} &= \tan\left(\varphi \pm \tfrac{\delta}{2}\right), \\ v_{CL} &= 0. \end{aligned} \tag{21}$$

In this case the trajectories follow the real axis for any value of the azimuth angle of the linear input polarization. And, since their position along the u axis is given by Eq. (21), for a fixed increment of the azimuth angle of the input linear polarization, the location on the real axis of the output polarization state does not present a uniform displacement [9].

Elliptical input polarization

The Cartesian equations and loci of invariant-ellipticity states have already been reported for this complex plane representation by Azzam and Bashara [16]. These trajectories do not correspond to those discussed here since they do not include linear or circular polarization states.

5. Elliptical birefringence

The birefringence matrix of an elliptical retarder is:

$$M_E = \begin{bmatrix} \cos\left(\frac{\delta}{2}\right) + i\sin\left(\frac{\delta}{2}\right)\cos 2\varepsilon\cos 2\alpha & \sin\left(\frac{\delta}{2}\right)(\sin 2\varepsilon + i\cos 2\varepsilon\sin 2\alpha) \\ -\sin\left(\frac{\delta}{2}\right)(\sin 2\varepsilon - i\cos 2\varepsilon\sin 2\alpha) & \cos\left(\frac{\delta}{2}\right) - i\sin\left(\frac{\delta}{2}\right)\cos 2\varepsilon\cos 2\alpha \end{bmatrix}, \tag{22}$$

where δ is the retardation angle between the polarization eigenmodes, ε is the birefringence ellipticity angle and α is the azimuth angle of the fast birefringence axis [3,10,11].

Circular input polarization

The output polarization state obtained using Eqs. (6), (7) and (22) is

$$V_{EC} = \begin{bmatrix} \cos\left(\frac{\delta}{2}\right) + i\sin\left(\frac{\delta}{2}\right)\cos 2\varepsilon\cos 2\alpha \mp i\sin\left(\frac{\delta}{2}\right)(\sin 2\varepsilon + i\cos 2\varepsilon\sin 2\alpha) \\ -\sin\left(\frac{\delta}{2}\right)(\sin 2\varepsilon - i\cos 2\varepsilon\sin 2\alpha) \mp i\left[\cos\left(\frac{\delta}{2}\right) - i\sin\left(\frac{\delta}{2}\right)\cos 2\varepsilon\cos 2\alpha\right] \end{bmatrix}. \tag{23}$$

In this case the values determined for u and v are

$$u_{EC} = \mp\frac{2\cos 2\varepsilon\sin\left(\frac{\delta}{2}\right)\left(\cos 2\alpha\cos\left(\frac{\delta}{2}\right) + \sin 2\alpha\sin 2\varepsilon\sin\left(\frac{\delta}{2}\right)\right)}{1 \pm 2\cos 2\varepsilon\sin\left(\frac{\delta}{2}\right)\left[\sin 2\alpha\cos\left(\frac{\delta}{2}\right) - \cos 2\alpha\sin 2\varepsilon\sin\left(\frac{\delta}{2}\right)\right]},$$

$$v_{EC} = \mp\frac{1 - 2\cos^2 2\varepsilon\sin^2\left(\frac{\delta}{2}\right)}{1 \pm 2\cos 2\varepsilon\sin\left(\frac{\delta}{2}\right)\left[\sin 2\alpha\cos\left(\frac{\delta}{2}\right) - \cos 2\alpha\sin 2\varepsilon\sin\left(\frac{\delta}{2}\right)\right]}. \tag{24}$$

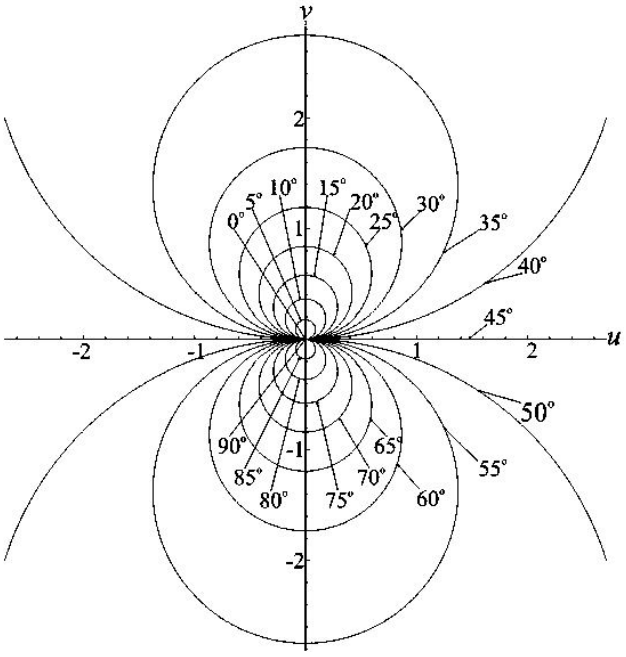

FIGURE 6. Elliptical retarders aligned with the laboratory reference frame illuminated with a signal with a horizontal linear input polarization ($\alpha = \varphi = 0°$). The retarder ellipticity angle varies from 0 to 90°.

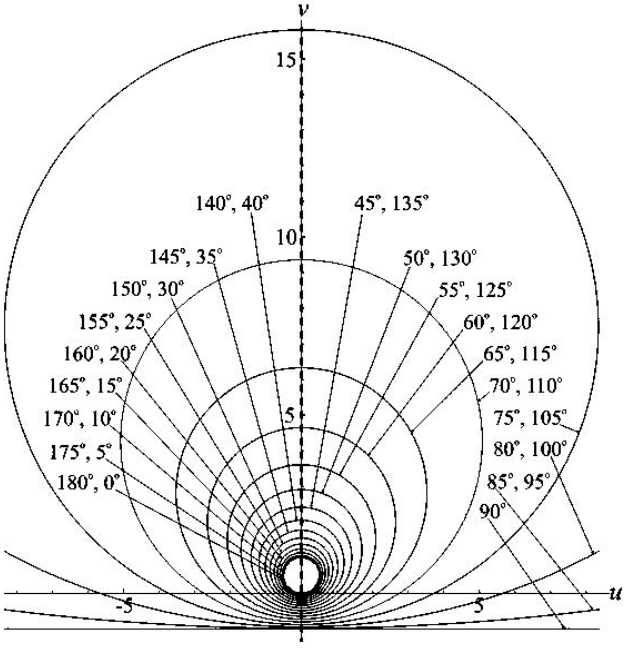

FIGURE 7. Elliptical retarder with ellipticity angle ε = 22.5° aligned with the laboratory reference frame and illuminated with a linearly polarized input signal. The azimuth φ of the input linear polarization varies from 0 to 90°.

To observe how the trajectory is modified when the azimuth angle of fast birefringence axis α (sample orientation) or when the ellipticity angle ε associated with the sample birefringence has a different value, we considered that only one of these parameters is modified. The results are presented in Figs. 4 and 5.

The radii of curvature and the centers of this family of circles satisfy

$$r_{EC} = \frac{1}{\tan 2\varepsilon - \cos 2\alpha} \tag{25}$$

and

$$(h,k)_{EC} = \left(\frac{\sin 2\alpha \cos 2\varepsilon}{\cos 2\alpha \cos 2\varepsilon - \sin 2\varepsilon}, \ \frac{\sin 2\varepsilon}{\cos 2\alpha \cos 2\varepsilon - \sin 2\varepsilon} \right). \tag{26}$$

We can notice from Eq. (25) that for a circular input signal the denominator is null when the fast birefringence axis of the sample is aligned with the reference frame (α = 0°) and the ellipticity angle of the sample is ε = 22.5°. In this case the radius of the circular path is infinite, *i.e* it includes the vertical state of polarization. Fig. 4 shows the trajectories obtained for an elliptical retarder with $0° < \varepsilon < 90°$; we can observe that the centers of these circumferences lie on the imaginary axis.

In agreement with Eq. (25), when the sample is aligned with the reference frame the singularity obtained for ε = 22.5° shifts to a different position (see Fig. 5). In this case, for α = 90° the diameter of the circle is unitary and its center is located on the v axis. As α increases from 0 to 90°, the radius decreases, while from 90 to 180° it grows with α. The centers of symmetry of these circumferences have negative u coordinates for $0 < \alpha < 90°$ and they become positive for $90° < \alpha < 180°$. For this family of circles the evolute is located out of the coordinate axes, not as a straight line but as a parabola with the input polarization state (0,-1) located at its focus (shown as a dashed line in Figs. 5a and 5b) Another interesting characteristic of this family of circles is that for any $\alpha \neq 0°$, the real axis behaves as an envelope that is also the directrix of the parabola associated with the evolute. All these circles are located below the real axis and each of them is tangent to the real axis (Figs. 5a and 5b). The states of polarization above the real axis are included in the trajectories having a right circular polarization as input polarization state. It is important to notice that each of these circles corresponds to a different retarder (different ellipticity angle ε).

Linear input polarization

Applying Eqs. (7), (12) and (22) to an elliptical retarder and a linear input polarization, we obtain the following output polarization:

$$V_{EL} = \begin{bmatrix} \left[\cos\left(\frac{\delta}{2}\right) + i \sin\left(\frac{\delta}{2}\right) \cos 2\varepsilon \cos 2\alpha\right] \cos\varphi + \sin\left(\frac{\delta}{2}\right) (\sin 2\varepsilon + i \cos 2\varepsilon \sin 2\alpha) \sin\varphi \\ -\sin\left(\frac{\delta}{2}\right) (\sin 2\varepsilon - i \cos 2\varepsilon \sin 2\alpha) \cos\varphi + \left[\cos\left(\frac{\delta}{2}\right) - i \sin\left(\frac{\delta}{2}\right) \cos 2\varepsilon \cos 2\alpha\right] \sin\varphi \end{bmatrix}. \tag{27}$$

When a linear input signal is used we have an additional parameter, the azimuth angle of the linear input polarization φ. From Eq. (27) and relation 4 it can be shown that

$$u_{EL} = \frac{\cos^2\left(\frac{\delta}{2}\right) \left[\frac{1}{2} \sin 2\varphi \cos\left(\frac{\delta}{2}\right) - \cos 2\varphi \sin 2\varepsilon \sin\left(\frac{\delta}{2}\right)\right] + \frac{1}{2} \sin^2\left(\frac{\delta}{2}\right) \left[\cos^2 2\varepsilon \sin\left[2\left(\alpha - \varphi\right)\right] - \sin 2\varphi \sin^2 2\varepsilon\right]}{cos^2(2\alpha - \varphi) \cos^2 2\varepsilon \sin^2(\frac{\delta}{2}) + [\cos\varphi \cos(\frac{\delta}{2}) + \sin\varphi \sin 2\varepsilon \sin(\frac{\delta}{2})]^2},$$

$$v_{EL} = \frac{\cos 2\varepsilon \left\{\sin\left[2\left(\alpha - \varphi\right)\right] \cos\left(\frac{\delta}{2}\right) + \cos\left[2\left(\alpha - \varphi\right)\right] \sin 2\varepsilon \sin\left(\frac{\delta}{2}\right)\right\} \sin\left(\frac{\delta}{2}\right)}{\cos^2(2\alpha - \varphi) \cos^2 2\varepsilon \sin^2(\frac{\delta}{2}) + [\cos\varphi \cos(\frac{\delta}{2}) + \sin\varphi \sin 2\varepsilon \sin(\frac{\delta}{2})]^2}. \tag{28}$$

The radii of curvature and the centers of this family of circles are given by:

$$r_{EL} = \frac{\sqrt{1 - \left\{\cos 2\varepsilon \cos\left[2\left(\alpha - \varphi\right)\right]\right\}^2}}{2 \cos\varphi \cos 2\varepsilon \cos\left(2\alpha - \varphi\right)} \tag{29}$$

$$(h,k)_{EL} = \frac{1}{2 \cos\varphi \cos\left(2\alpha - \varphi\right)} \left(\sin 2\alpha, \tan 2\varepsilon\right) \tag{30}$$

To show the role of the various parameters, we have simulated the trajectories described by the evolution of the polarization state of a linear input signal modifying one parameter at a time as follows:

i) When the fast birefringence axis of the sample is aligned with the reference system and the input linear polarization is horizontal, the trajectories depicted by the evolution of the signal's polarization state are circles centered on the imaginary axis (Fig. 6). Using Eq. (29) it can be shown that in this case the circle radius depends only on the value of the sample ellipticity angle, $r = 1/2 \tan 2\varepsilon$. Therefore, the trajectory radius is equal to zero when ε = 0° (linear birefringence); for $0 \leq \varepsilon \leq 45°$ it grows with ε and goes off to infinity when ε = 45° (circular birefringence).

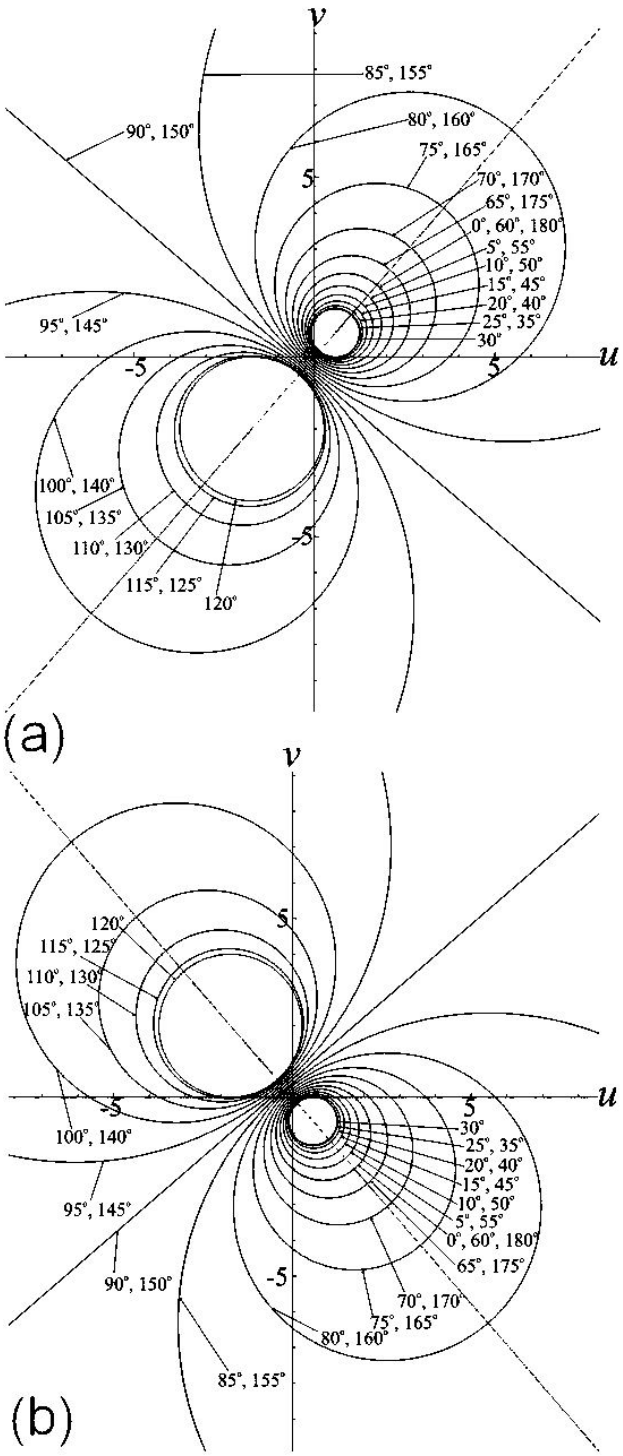

FIGURE 8. a) Elliptical retarder with ellipticity angle $\varepsilon = 22.5°$ illuminated with a linear input polarization and $\alpha = 30°$. The azimuth φ of the input linearly polarized signal varies from 0 to 90°. b) Elliptical retarder with ellipticity angle $\varepsilon = 22.5°$ illuminated with a linear input polarization and $\alpha = 120°$. The azimuth ϕ of the linear input signal varies from 0 to 90°.

ii) If we keep the sample aligned with the reference system ($\alpha = 0°$) but allow the azimuth angle of the input linear polarization to change, the centers of symmetry of the resultant trajectories remain on the imaginary axis but, since the input polarization state is displaced along the real axis, the distribution of these trajectories is different (Fig. 7). When the orientation of the input signal (φ) changes, the circles' radii grow with this angle and for $\varphi = 90°$ (vertical polarization) the value of the radius goes off to infinity. Since we are using linear input polarization to calculate the circular path, depending on the ellipticity angle of the elliptical retarder (ε), there is a circle surrounding the polarization eigenmode of the sample of polarization states. It will not form part of any trajectory.

iii) If the birefringence axes of the sample are no longer aligned with the reference system, the centers of curvature are located on a straight line passing through the origin.

As we can see in Fig. 8, when $\varepsilon = 22.5°$ and $\alpha = 30°$, the loci of the centers of the family of circles (evolute) obtained for $0 < \varphi < 90°$ (dashed line in Fig. 8a) form a straight line with a 45° slope (equal to tan 2ε). Comparing these results with those obtained for $\alpha = 120°$ (Fig. 8b) it becomes evident that the slope of the evolute is modified when the azimuth angle of the fast birefringence axis is greater than 90°. In this case the entire diagram presents a 90° rotation in a clockwise direction. We should also notice that under these conditions, the value of the radius goes off to infinity for $\varphi = 90°$.

iv) For a specific retarder, the ellipticity angle remains fixed if we keep the azimuth angle of the linear input polarization constant, and vary the orientation of the sample (α); the evolute of the new family of circles is a hyperbola asymptotic to two straight lines crossing the origin (Figs. 9a and 9b). The absolute value of the slope of these straight lines is equal to —tan 2ε—. In Fig. 9a, $\varepsilon = 22.5°$, $\varphi = 0$ and $0 < \alpha < 180°$. Under these experimental settings, the envelope of this family of circles is a Lemniscate of Bernoulli. An amplification of this envelope (Fig. 9b) shows its axis is aligned with the imaginary axis.

The states of polarization inside Bernoulli's Lemniscate are again elliptical polarization states located close to the polarization eigenmodes of this sample that cannot be reached when the trajectory includes a linear state of polarization.

6. Summary

We derived analytical expressions for the trajectories depicted by the evolution of the polarization of light in the complex plane of polarization, when it travels along a homogeneous retarder (linear, circular or elliptical). The resulting complex plane is the stereographic projection of the 3D Poincaré sphere [7,10-12]; therefore these circular trajectories validate the analytical expressions presented here.

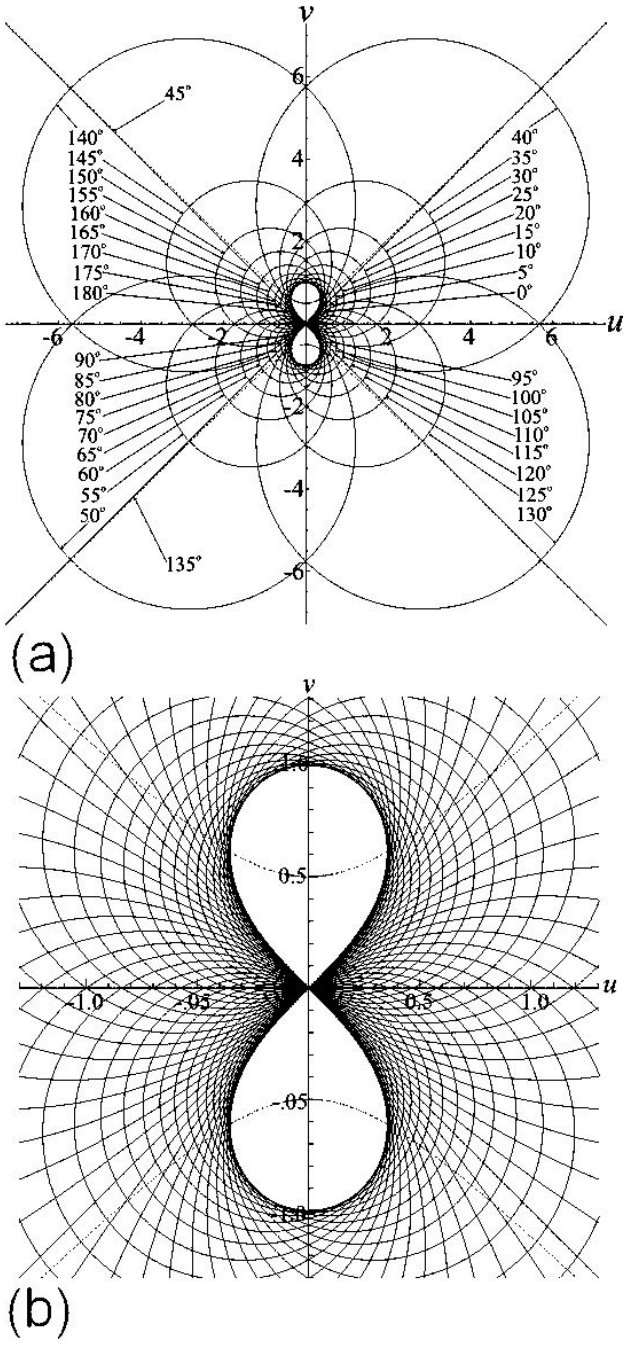

FIGURE 9. a) Elliptical retarder with an ellipticity angleε = 22.5° illuminated with a linearly polarized input signal with azimuth angle φ = 0°. These trajectories correspond to different values of the azimuth angle (α) of the fast birefringence axis of the sample (0 to 90°). The centers of the circular trajectories are located along a curve asymptotic to a straight line whose slope is equal to tan2ε. b) It is a magnification of Fig. 9a, it shows with a better detail that the evolute of this family of circles corresponds to the two branches of a hyperbola aligned with the imaginary axis. It can also be noticed that its envelope is a Lemniscate of Bernoulli

We have ascertained that the use of these relations improves the utility of this planar chart method. Our results can be used 1) to identify from experimental data the type of anisotropy of the homogeneous retarder or 2) to model the evolution of light polarization when the input or the output polarization states are either linear or circular (typical input and/or output polarization states).

To identify the type of anisotropy, in this study we show that for a linear retarder the circular trajectories depicted by the evolution of the input polarization state (linear or circular) are always centered on a point located on the real axis. We calculated the equations relating the value of the radius and the locus of the center of curvature to the sample orientation and the input polarization state of the signal. For a circularly polarized input signal, the value of the radius and its locus on the real axis depend on the sample orientation with respect to the reference frame used to measure the state of polarization. When the input signal is linearly polarized, the radii of the resulting family of circles and its evolute depend on the sample orientation and on the azimuth angle of the input signal.

For a circular retarder the result is quite different. Since right and left circular polarizations correspond to the polarization eigenmodes, for a circularly polarized input signal the polarization state remains unchanged; the trajectory depicted on the complex plane is just a point located at (0,$\pm$1). For a linearly polarized signal the trajectory is a straight line along the real axis.

For a sample with an elliptical birefringence, the evolution of the polarization state of a linearly or circularly polarized input signal depict also a circular trajectory, but in this case the evolute of this family of circles is located outside of the real axis. For a circularly polarized input signal the radius and center of curvature of each circle depend on the sample ellipticity and orientation, and for a linearly polarized signal they depend as well on the azimuth angle of the input signal. When the sample is aligned with the reference system and the input signal is circularly or linearly polarized, the center of the circular trajectory described as its polarization evolves, lying on the imaginary axis. When the fast birefringence axis of the sample has a non-zero azimuth angle, the center of the trajectory has non-zero u and v coordinates for a circular or a linear input polarization. For a circularly polarized input signal, the evolute of the resultant family of circles is a parabola whose focus is located at the point associated with the input state of polarization. If the input signal is linearly polarized, varying the azimuth angle of the linear input polarization, the evolute is a straight line crossing the origin of the complex plane with slope equal to the absolute value of tan 2ε (ε being the ellipticity angle of the sample). If the input linear signal is kept fixed and the orientation of the sample with respect to the reference system is varied, the evolute of the resultant family of circles is a hyperbola aligned with the imaginary axis.

A disadvantage to this graphic method is that for any homogeneous retarder we have found practical conditions for which the state of polarization will not be defined (it goes off to infinity). However, this condition can be modified by changing the sample orientation or the input state of polarization. The main advantage to this planar graphic repre-

sentation is that it can be applied to coherent systems (devices) since it makes use of the Jones matrix formalism. It should also be mentioned that this representation keeps the symmetry properties of other graphical representations [4] and, since it is based on polarization states, eludes the practical limitations introduced by non-ideal coupling presented by polarimetric methods based on intensity measurements, where *a priori* knowledge of the sample birefringence is required [18].

7. Conclusions

In this work we calculated the trajectories depicted by the evolution of the polarization state for homogeneous retarders, using the Jones formalism and a complex plane representation. For any homogeneous retarder these trajectories are families of circles whose radius and evolutes have been related with the birefringence and orientation of the sample, and the state of polarization of the input signal. The analytical models presented here allow, the behavior of the state of polarization of light as it propagates along the sample (fiber, nematic liquid crystal) to be visualizing on a flat plane. They can be used for design purposes or for the identification of the sample anisotropy when it behaves as a homogeneous retarder.

Acknowledgements

This work was supported by CONACYT through the scholarship granted to César Ayala Díaz.

1. M. Smith, *J.Phys. E: Scientific Instruments* **12**(1979) 927.
2. A.J. Barlow, *J. Lightwave Technol.* **3** (1985) 135.
3. C. Tsao, *Optical Fibre Waveguide Analysis* (Oxford University Press, 1992).
4. R.M. Azzam and N.M. Bashara, *Opt. Commun.* **5** (1972) 319.
5. R.M. Azzam, B.E. Merrill, and N.M. Bashara, *Appl. Opt.* **12** (1973) 764.
6. F. Treviño-Martínez, D. Tentori, C. Ayala-Díaz, and F.J. Mendieta-Jiménez, *Opt. Express* **13** (2005) 2556.
7. H.G. Jerrard, *J. Opt. Soc. Am.* **44** (1954) 634.
8. R.M.A. Azzam and N.M. Bashara, *J. Opt. Soc. Am.* **62** (1971) 222.
9. R.M.A. Azzam and N.M. Bashara, *Appl. Phys.* **2** (1973) 59.
10. D.S. Kliger, J.W. Lewis, and C.E. Randall, *Polarized light in optics and spectroscopy* (Academic Press, 1990).
11. E. Collett Polarized light. *Fundamentals and applications* (Marcel Dekker, 1993).
12. S. Huard, *Polarization of Light* (John Wiley& Sons, 1997).
13. T. Okoshi, *J. Lightwave Technol.* **4** (1986) 1367.
14. K.K. Tedjojuwono, W.W. Hunter Jr., and S.L. Ocheltree, *Appl. Opt.* **28** (1989) 2614.
15. H.G. Venkatesh and G.G. Sarkar, *J. Phys. A* **9** (1976) 1015.
16. M.A. Kashan, *Opt. Acta* **31** (1984) 1345.
17. R.M.A. Azzam and N.M. Bashara, *Appl. Opt.* **12** (1973) 62.
18. K. Kikuchi and T. Okoshi, *Opt. Lett.* **8** (1983) 122.